SIMULATION OF PHYSICAL PROCESSES

Conference materials
UDC 537.9, 544.47, 004.94
DOI: https://doi.org/10.18721/JPM.153.111

Atomic and electronic structure of $YFeO_3$ surface with oxygen vacancies

A. A. Gnidenko [1] ✉, P.G. Chigrin [1]

[1] Institute of Materials of Far Eastern Branch of the RAS, Khabarovsk, Russia

✉ agnidenko@mail.ru

Abstract: The atomic and electronic structure of $YFeO_3$ surfaces at the formation of oxygen vacancies are investigated by the methods of quantum-mechanical calculations. The (100), (001), and (010) surfaces are considered. The dependence of the formation energy of surface oxygen vacancy on its concentration and type of surface is shown. (100) surface oxygen vacancy has the lowest formation energy. During the formation of vacancies on the surface, the 3*d* states of Fe split into bulk, surface, and near-surface states.

Keywords: density functional theory, pseudopotential method, surface effects, yttrium orthoferrite, oxygen vacancies

Citation: Gnidenko A. A., Chigrin P. G. Atomic and electronic structure of $YFeO_3$ surface with oxygen vacancies. St. Petersburg State Polytechnical University Journal. Physics and Mathematics. 15 (3.1) (2022) 65–70. DOI: https://doi.org/10.18721/JPM.153.111

Материалы конференции
УДК 537.9, 544.47, 004.94
DOI: https://doi.org/10.18721/JPM.153.111

Атомная и электронная структура поверхности $YFeO_3$ с кислородными вакансиями

А. А. Гниденко [1] ✉, П. Г. Чигрин [1]

[1] Институт материаловедения Хабаровского научного центра Дальневосточного отделения РАН, г. Хабаровск, Россия

✉ agnidenko@mail.ru

Аннотация. Атомная и электронная структура поверхности $YFeO_3$ при формировании кислородных вакансий исследована при помощи квантово-механических методов моделирования. Рассмотрены поверхности (100), (001) и (010). Продемонстрирована зависимость энергии формирования кислородных вакансий от их концентрации и типа поверхности. С наименьшими энергетическими затратами кислородные вакансии формируются на поверхности (100). При формировании вакансий на поверхности происходит расщепление 3*d*-состояний Fe на объемные, поверхностные и приповерхностные.

Ключевые слова: теория функционала плотности, метод псевдопотенциалов, поверхностные эффекты, ортоферрит иттрия, кислородные вакансии

Ссылка при цитировании: Гниденко А. А., Чигрин П. Г. Атомная и электронная структура поверхности $YFeO_3$ с кислородными вакансиями // Научно-технические ведомости СПбГПУ. Физико-математические науки. 2022. Т. 15. № 3.1. С. 65–70. DOI: https://doi.org/10.18721/ JPM.153.111

Introduction

In the last two decades, complex oxides with a perovskite structure (ABO_3) have become the subject of intensive research over the world [1, 2]. The field of application of these materials is very wide: various types of sensors and detectors, solar cells, photocatalysts and solid oxide fuel cells [3–6]. The functional properties of these compounds are mostly determined by stoichiometry and structural changes within ABO_3 [7]. It was found that defect formation in the crystal lattice of ABO_3 leads to a significant increase in catalytic activity [8], while the oxygen non-stoichiometry of $YFeO_{3-\delta}$ can reach $\delta = 0.25$ [9]. A lot of research has been dedicated to developing perovskite catalysts for redox reactions such as the oxidation of hydrocarbons, soot and carbon monoxide. Thus, perovskite compounds can be used as alternative multifunctional catalysts for neutralizing diesel gases.

The mechanism of carbon oxidation in the presence of catalysts with a perovskite structure has not been comprehensively explored this far. It should be noted that vacancies on the perovskite surface are filled with oxygen from the bulk of the crystal. Thus, the influence of the structural characteristics of perovskite on the mobility, surface/volume reactivity of oxygen, and catalytic activity in carbon oxidation is of great interest for fundamental research. In the present work, yttrium orthoferrite ($YFeO_3$) was considered; the atomic and electronic structure of this perovskite at the formation of oxygen vacancies on the surface was studied using modern computer simulation methods.

Methods and Calculation Parameters

The Quantum Espresso software package [10], based on the density functional theory [11, 12] and the pseudopotential method, was used to perform quantum mechanical calculations. The exchange-correlation contribution to the total energy was described by the generalized gradient approximation. Uniform k-point grids were specified by Monkhorst-Pack procedures and varied depending on the size of the supercell. Cutoff energy of the plane wave basis was about 816 eV. Ultrasoft pseudopotentials for yttrium, iron, and oxygen were taken from the Quantum Espresso pseudopotential database [13] and were tested for a correct description of the properties of the Y and Fe crystal lattices, as well as of the O_2 molecule.

$YFeO_3$ has an orthorhombic primitive cell (*Pnma* space group); according to our calculation, the lattice parameters are $a = 5.65$ Å, $b = 7.64$ Å, $c = 5.29$ Å; deviation from the experimental values is less than 1%. ABO_3 perovskites (where B = Fe) are often antiferromagnets; the equilibrium configuration for $YFeO_3$ corresponds to the G-type antiferromagnetic state, which is consistent with the literature data. Furthermore, Hubbard correction (DFT + U) [14] was applied into the calculations with $U_{eff} = 4$ eV for adequate description of strongly localized $3d$-states of Fe.

Results and Discussion

A primitive orthorhombic cell of $YFeO_3$ was taken to construct the slab models. It contains 4 structural units (20 atoms in total). For simplicity of construction, we considered the facets of the primitive cell, thus we obtained surfaces with indices (001), (010) and (100). To estimate the surface energy of non-stoichiometric slab we calculated a difference between the slab energy before ($E_{unrel.slab}$) and after ($E_{rel.slab}$) atomic relaxation, reduced to a unit of surface area (S):

$$E_{surf} = \frac{E_{unrel.slab} - E_{rel.slab}}{2S}. \quad (1)$$

We considered an asymmetric slab: the lower atomic layers were fixed. Fig. 1 shows the slab where only the middle atomic layers are fixed, before (*a*) and after (*b*) relaxation, as well as the slab with fixed lower atomic layers after relaxation (*c*). Fe atoms in Fig. 1 and 2 are marked in dark grey, Y atoms in light gray, and O atoms in white. Atomic structure analysis showed that the bond lengths in the surface layers after relaxation in both cases coincide with an accuracy of 0.01 Å. The surface energy for the slab with fixed lower layers was determined by a formula similar to (1), but without a factor of 2 in the denominator, since only one (upper) surface is considered. The vacuum gap in our calculations was about 14 Å. The calculated values of surface energies are given in Table 1.

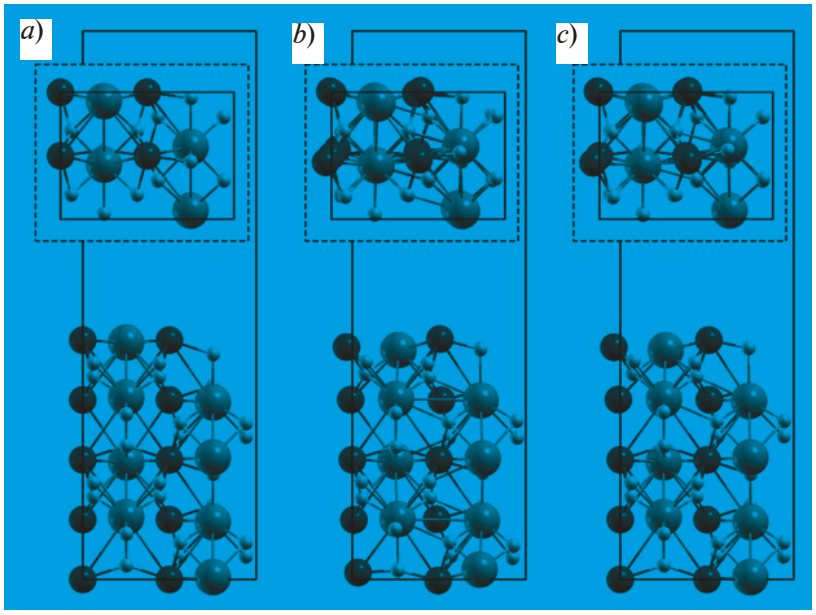

Fig. 1. Slab for the $YFeO_3$ (001) surface in two projections: before relaxation (*a*); after relaxation of the upper and lower atomic layers (*b*); after relaxation of only the upper atomic layers (*c*)

Table 1

Surface energies of $YFeO_3$ (001), (010) and (100)

Surface	Area, m^2	Slab characteristics	Surface energy, J/m^2
(001)	$4.36 \cdot 10^{-19}$	5 layers	0.92
		7 layers	0.91
		5 layers, the lower layers are fixed	0.97
(010)	$3.01 \cdot 10^{-19}$	9 layers (FeO_2)	1.03
		9 layers (YO)	1.31
		9 layers (FeO_2), the lower layers are fixed	1.05
(100)	$4.11 \cdot 10^{-19}$	5 layers	1.06
		5 layers, the lower layers are fixed	1.11

For the (001) surface, the influence of the number of atomic layers on surface energy was estimated. It had been shown that the difference in surface energy between 5- and 7-layer slabs is only 0.01 J/m^2. The fixation of the lower atomic layers leads to an insignificant (within 0.05 J/m^2) increase in the surface energy, which indicates that the approach we have chosen is acceptable. The same results for slabs with fixed lower layers were obtained for $YFeO_3$(100) and $YFeO_3$(010). The number of layers in the (010) slab is 9, because in this direction, the linear size of the unit cell is larger. Additionally, the atomic layers for the direction [010] consist of either Fe and O atoms or Y and O atoms. Our calculations showed that formation of a (FeO_2) surface is more favorable; the energy difference is 0.3 J/m^2. Further, we considered only this type of surface.

In the simplest approximation, taking the chemical potential of oxygen as half the O_2 molecule total energy, the formation energy of a surface vacancy is determined as follows:

$$E_{form} = E_{slab+vac} - E_{slab} + \frac{1}{2}E_{O_2}, \quad (2)$$

where E_{slab} is the energy of the $YFeO_3$ slab, $E_{slab+vac}$ is the energy of the slab with oxygen surface vacancy, E_{O_2} is the energy of an isolated O_2 molecule. The obtained values are shown in Table 2.

For each surface, we considered two cases, which differed from each other by the

Table 2

Energies of oxygen vacancy formation for different types of $YFeO_3$ surfaces

Surface	Area, m^2	E_{form}, eV
(001)	$4.36 \cdot 10^{-19}$	2.40
	$17.45 \cdot 10^{-19}$	1.74
(100)	$4.11 \cdot 10^{-19}$	1.79
	$16.44 \cdot 10^{-19}$	0.81
(010)	$3.01 \cdot 10^{-19}$	3.51
	$12.03 \cdot 10^{-19}$	3.33

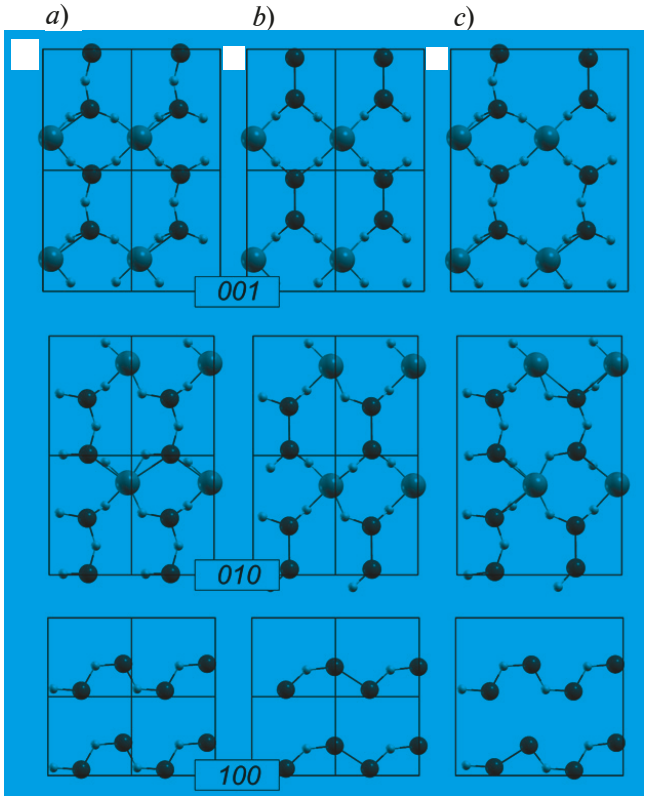

Fig. 2. Atoms of $YFeO_3$ surface layers: without oxygen vacancy (*a*); one vacancy per unit cell cross-section (*b*); one vacancy per cell area increased by 4 times(*c*)

cross-section area. In contrast to the description of bulk oxygen vacancies, we cannot operate in terms of oxygen non-stoichiometry; therefore, below we consider high and low concentrations of surface oxygen vacancies. Fig. 2 shows the atoms forming the surface layer for (001), (100), and (010); the second and third images in each row correspond to high and low vacancy concentrations. To create a vacancy on the surface, we removed the oxygen atom with the highest position in the direction of the slab orientation; for all surfaces, it was an oxygen atom from the Fe-O-Fe bridge. Thus, the formation of an oxygen vacancy leads to the formation of a Fe-Fe bond on the surface (its length varies from 2.62 to 2.82 Å).

It was found that the formation energy of a surface oxygen vacancy decreases with an increase in the cross-section area, i.e., a decrease in the vacancy concentration. Due to the specific arrangement of atoms on the $YFeO_3$(010) surface layer, the formation energies do not differ too much from previously calculated values for bulk oxygen vacancies (3.13–3.79 eV) [15]. However, the vacancy formation energies were significantly lower for the (001) and (100) surfaces; in the case of low concentration on the (100) surface, the lowest value was obtained, amounting to 0.81 eV. For more detailed analysis, we plotted the density of electronic states (DOS) for all considered cases.

The left side of Fig. 3 shows the total and projected densities of electronic states for an ideal $YFeO_3$ cell and a cell with an oxygen vacancy (with high and low concentration). The Fermi level is at zero. The formation of an oxygen vacancy leads to appearance of levels in the band gap, as well as to partial delocalization of 3*d* states of Fe; in the case of high concentrations this is more pronounced. At the vacancy formation on the $YFeO_3$ (010) surface (right panel in Fig. 3), it is noticeable that, in addition to the sharp peak at −8 eV corresponding to 3*d* states of bulk Fe atoms, there are distributed states (in the range from −7 eV to −6 eV) corresponding to surface Fe atoms. In the case of the (001) and (100) surfaces (Fig. 4), there is a partial splitting of the peak corresponding to the bulk states; it becomes the superposition from the states of the bulk and near-surface Fe atoms. This occurs due to formation of the Fe-Fe bond when oxygen is removed from the surface and the surface layers are included in the atomic relaxation process.

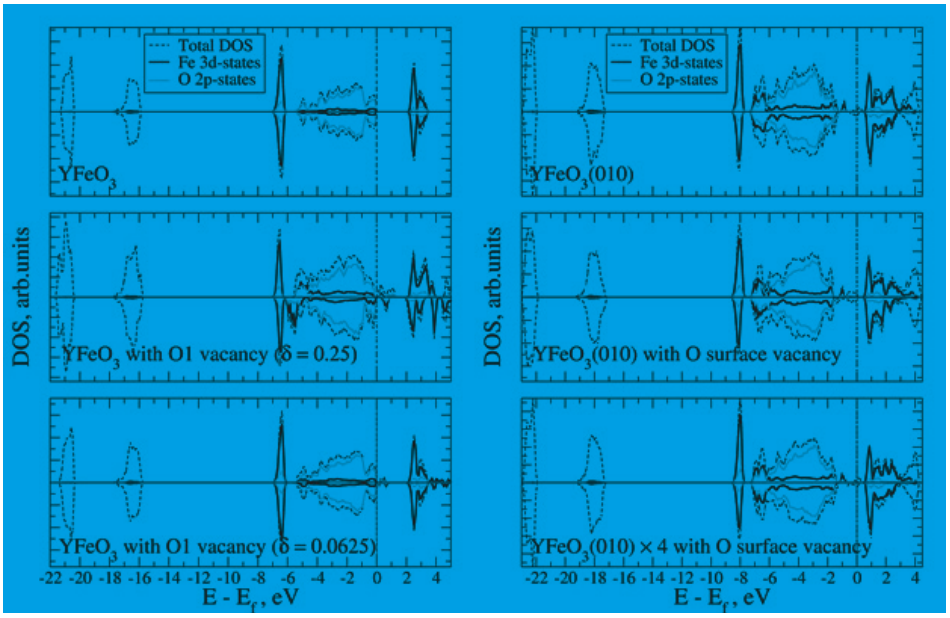

Fig. 3. Densities of electronic states for $YFeO_3$ and $YFeO_3$(010) surface in the absence and presence of oxygen vacancies

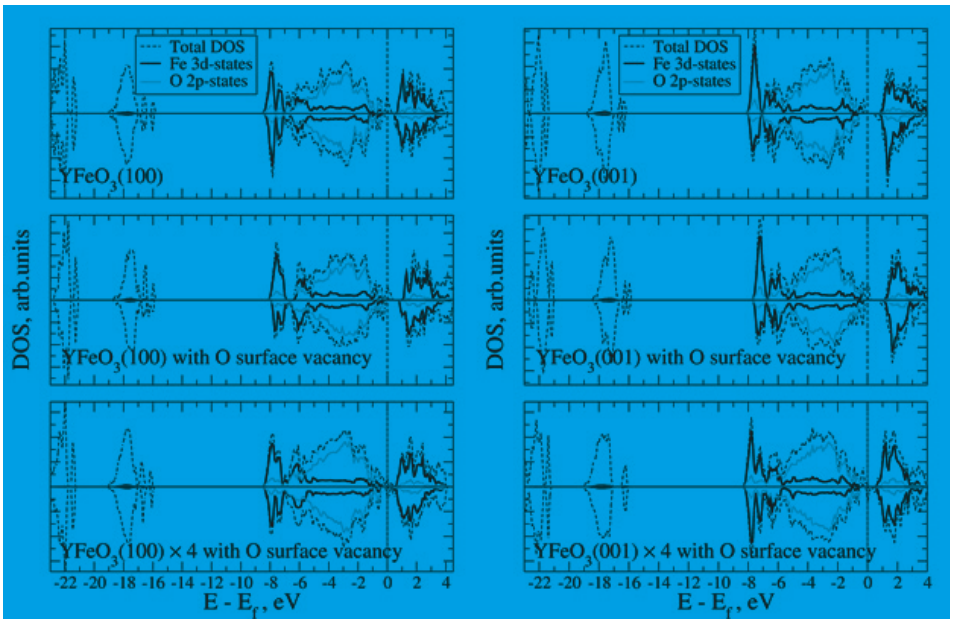

Fig. 4. Densities of electronic states for $YFeO_3$(100) and $YFeO_3$(001) surfaces in the absence and presence of oxygen vacancies

Conclusion

Computer simulation methods have been used to study changes in the atomic and electronic structure upon formation of oxygen vacancies on different surfaces of yttrium orthoferrite. It was found that there is a tendency to a decrease in the formation energy with an increase in the surface area, which corresponds to a decrease in the vacancy concentration. The smallest value of 0.81 eV was obtained for the (100) surface, which is about four times less than the formation energy of a bulk oxygen vacancy. Analysis of the electronic structure showed delocalization of 3*d* states of Fe atoms for the surface formation process; the formation of an oxygen vacancy enhances this effect due to the appearance of Fe-Fe bond.

Acknowledgments

This research was supported by the computational resources provided by the *Akademik V.M. Matrosov* HPC-cluster (Irkutsk) [16].

REFERENCES

1. **Li Ch. H., Ch K., Soh K., Wu P.,** Formability of ABO_3 perovskites, J. Alloys Compd. 372 (2004) 40–48.

2. **Atta N. F., Galal A., El-Ads E. H.,** Perovskite Nanomaterials-Synthesis, Characterization, and Applications, in "Perovskite Materials Synthesis, Characterisation, Properties, and Applications". Edited by Likun Pan Guang Zhu, InTechOpen, 2016, pp. 648.

3. **Shi J., Guo L.,** ABO_3-based photocatalysts for water splitting, Progress in Natural Science: Materials International. 22 (2012) 592–615.

4. **Chroneos A., Vovk R. V., Goulatis I., Goulatis L. I.,** Oxygen transport in perovskite and related oxides: A brief review, J. Alloys Compd. 494 (2010) 190–195.

5. **Cui J., Wang J., Zhang X., Li G., Wu K., Cheng Y., Zhou J.,** Enhanced oxygen reduction reaction through Ca and Co co-doped $YFeO_3$ as cathode for protonic ceramic fuel cells, Journal of Power Sources. 413 (2019) 148–157.

6. **Moure C., Peca O.,** Magnetic features in $REMeO_3$ perovskites and their solid solutions (RE=rare-earth, Me=Mn, Cr), Journal of Magnetism and Magnetic Materials. 337-338 (2013) 1–22.

7. **Pena M., Fierro J.L.G.,** Chemical structures and performances of perovskite oxides, Chem. Rev. 101 (2001) 1981–2017.

8. **Barresi A. A., Mazza D., Ronchetti S., Spinicci R., Vallino M.,** Non-stoichiometry and catalytic activity in ABO_3 perovskites: $LaMnO_3$ and $LaFeO_3$, Studies in Surface Science and Catalysis. 130 (2000) 1223–1228.

9. **Dhal G. Ch., Dey S., Mohan D., Prasad R.,** Solution Combustion Synthesis of Perovskite-type Catalysts for Diesel Engine Exhaust GaS Purification, Materials Today: Proceedings. 4 (2017) 10489–10493.

10. **Giannozzi P., Baroni S., Bonini N., Calandra M., et al.,** QUANTUM ESPRESSO: a modular and open-source software project for quantum simulations of materials, J. Phys.: Condens. Matter. 21 (2009) 395502(19pp).

11. **Hohenberg P., Kohn W.,** Inhomogeneous Electron Gas, Phys. Rev. 136 (1964) B864–B871.

12. **Kohn W., Sham J.L.,** Self-Consistent Equations Including Exchange and Correlation Effects, Phys. Rev. 140 (1965) A1133–A1138.

13. **Corso A. Dal,** Pseudopotentials periodic table: From H to Pu, Comput. Mater. Sci. 95 (2014) 337–350.

14. **Anisimov V. I., Zaanen J., Andersen O. K.,** Band theory and mott insulators: Hubbard U instead of Stoner I. Phys. Rev. B. 44 (1991) 943–954.

15. **Gnidenko A.A., Chigrin P.G., Kirichenko E.A.,** Computer Simulation of Oxygen Vacancy Formation in $YFeO_3$ Perovskite, Solid State Phenomena. 312 (2020) 355–360.

16. Irkutsk Supercomputer Center of SB RAS, URL: http://hpc.icc.ru

THE AUTHORS

GNIDENKO Anton A.
agnidenko@mail.ru
ORCID: 0000-0002-9492-8429

CHIGRIN Pavel G.
pal_chig@mail.ru
ORCID: 0000-0002-1560-489X

Received 21.05.2022. Approved after reviewing 10.06.2022. Accepted 17.06.2022.